Plasma radiation losses in the electrostatic limit

Reuven Ianconescu

riancon@mail.shenkar.ac.il, riancon@gmail.com

Shenkar College of Engineering and Design

Abstract

Steady state ion drift configurations are usually treated as time independent problems, hence radiation losses are usually ignored. This assumption is not strictly true when the number of charge carriers is small and their acceleration is big. According to Larmor formula $q^2a^2/(6\pi\epsilon_0 c^3)$, accelerating charges radiate. In spite of that, even if single charges accelerate, in the continuum DC limit, there is no radiation. This challenge is encountered in any plasma application based on a steady state ion drift, because ions accelerate under the influence of the electric field. Even if we assume the model of an average speed, defined by the average gas mobility multiplied by the electric field, the velocity changes because the electric field is not constant in magnitude or direction. One remarks that in any curvilinear DC electric current path, charge carriers are accelerated, raising the question of when are radiation losses significant. This issue is best analyzed in a canonical configuration of charges in circular motion. One single charge simply radiates power according to Larmor formula. When distributing the charge over the circle, the destructive interference between the field contributions of the different charges, reduce the radiated power so that it goes to 0 in the continuum DC limit.

Key words: radiation, electrostatics, accelerating charges

PACS: 52.30.-q, 41.20.-q

1. INTRODUCTION

The radiation from an accelerating charge and the dumping force arising from it has a long history starting with from Dirac [1]. Knowing that an accelerating charge radiates energy according to Larmor formula, there must be a mechanism to supply this energy to the charge, working against a *dumping force*. This dumping force is sometimes called “self force” when one single charge is present, and it is equal to the differential energy loss along the charge’s path, divided by the path length dW/dl. This force is actually the Lorentz force $\bar{F} = q(\bar{E} + \bar{v} \times \bar{B})$, but when dealing with a point charge a natural problem arises from the fact that the fields $\bar{E}$ and $\bar{B}$ are infinite at the charge’s location. This inconsistency accompanies any single point charge problem, due to the fact that such charge has infinite energy. Several works [1–3] deal with this issue, and other works [4, 5] deal with collection of charges and mutual influences between the charges. This mutual influence needs to be profoundly investigated when one wants to understand the behavior of charges in the continuum DC limit. We know that in any curvilinear DC electric current path, charge carriers are accelerated, but in spite of that, the radiation is 0.

This brings us back to the old “paradox” of the unstable electron orbiting around the nucleus. When supposing that the electron orbits around the nucleus like the earth around the sun, the question which arose was why doesn’t it radiate its energy away according to the Larmor formula? This “paradox” is usually said to be solved by quantum mechanics, which showed that there are constant energy levels of the electron. This statement is partially true, but misses an important point. The Hamiltonian which led to this quantum solution did not contain any *dumping force* term, hence clearly one obtains constant energy solutions. The true reason is that in the quantum view, the electron is not localized, hence it exists with equal probability at any azimuthal angle around the nucleus, or in other words, makes a continuous DC current.

The objective of this work is to analyze by which mechanism the radiation from charges goes to 0 in the DC limit. The key to understand this phenomenon is the destructive interference and this issue is best analyzed in a canonical configuration of charges in circular motion. The current work is done in a non relativistic framework.

The configuration and the terminology are explained in Section 2. In Section 3 we calculate the fields and derive an expression for the radiated power, and in Section 4 we analyze the results and calculate some examples. The work is ended with some concluding remarks.

2. THE CONFIGURATION

The configuration is shown in Figure 1.

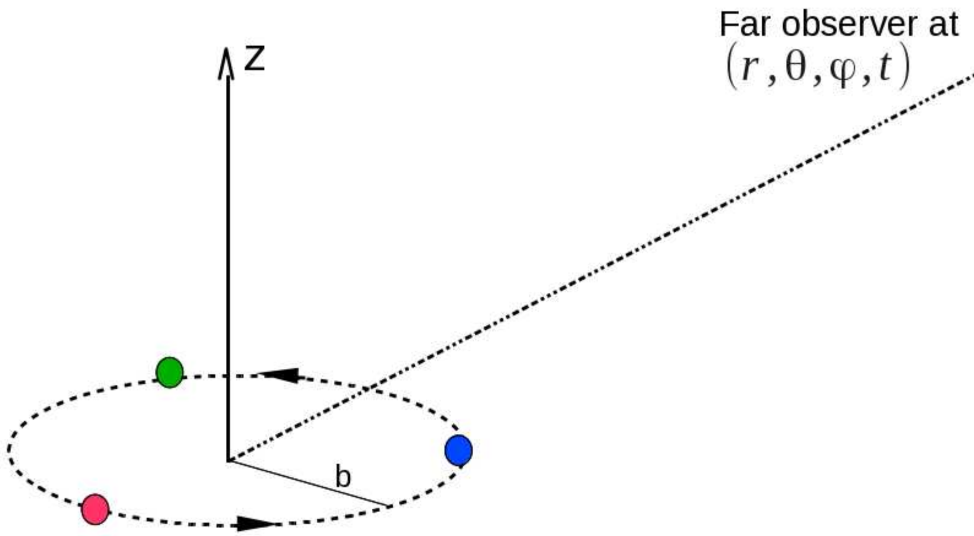

FIG. 1: (color online) Charges Q_k each one of charge q/N in circular motion on the xy plane at radius b around the z axis. Here k goes from 1 to 3.

There are N charges of magnitude q/N each, moving with constant speed v in a circular path of radius b, hence the angular velocity is $\omega = v/b$. The charges are uniformly distributed, so that the arc between two neighboring charges is $2\pi/N$ radians.

The location of the charge k as function of time is given by:

$$\bar{r}'_k(t) = b[\widehat{x}\cos(\omega t + 2\pi k/N) + \widehat{y}\sin(\omega t + 2\pi k/N)] \tag{1}$$

The fields propagate with the speed of light c. Hence the fields at the observer location $\bar{r}$ at time t are influenced by the motion of each charge, at an *earlier* (retarded) time. Specifically, the fields are influenced by the motion of the charge k at time t'_k so that

$$R_k \equiv |\bar{r} - \bar{r}'_k(t'_k)| = c(t - t'_k) \tag{2}$$

At large distance from the charges, one may approximate:

$$R_k \approx r - b\sin\theta\cos(\omega t'_k + 2\pi k/N - \varphi) \tag{3}$$

hence the retarded time t'_k may be calculated from the following implicit equation:

$$t'_k = t - r/c + (b/c)\sin\theta\cos(\omega t'_k + 2\pi k/N - \varphi). \tag{4}$$

Figure 2 emphasizes the meaning of retarded positions of the charges.

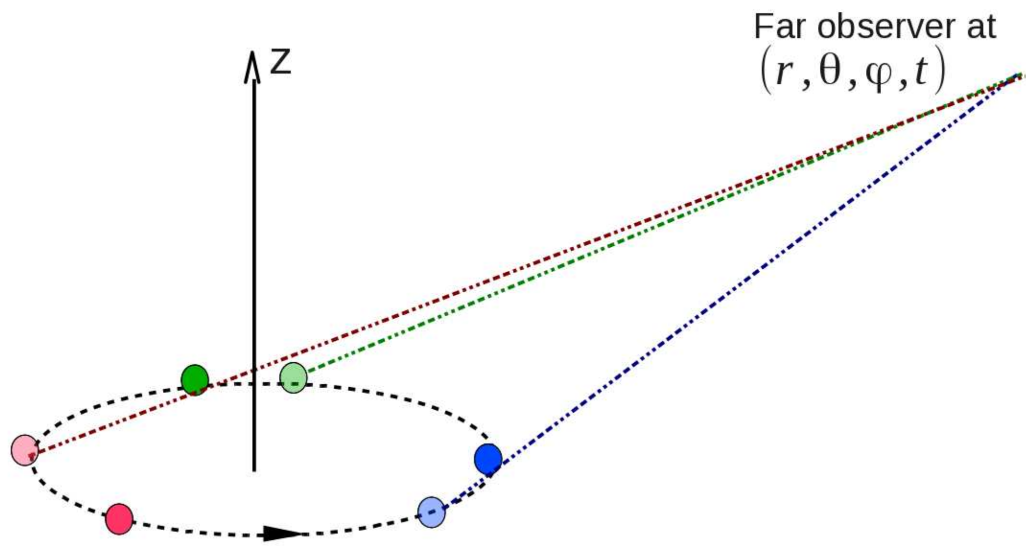

FIG. 2: (color online) The dark colored spheres show the charges at the current position at time t and the light colored spheres show the retarded positions at times t'_k. The retarded positions are connected with dashed lines to the observer location, emphasizing that the field at observer is determined by the charge's velocities and accelerations at the retarded times.

It is convenient to define

$$\phi_k \equiv \omega t'_k + 2\pi k/N - \varphi, \tag{5}$$

$$\varphi' \equiv \varphi - \omega(t - r/c) \tag{6}$$

and

$$p \equiv \beta\sin\theta \tag{7}$$

where $\beta \equiv \omega b/c = v/c$ is the charge's velocity relative to the light velocity c. Using the above, one may rewrite the implicit equation (4) as

$$\phi_k = -\varphi' + 2\pi k/N + \beta \sin\theta \cos\phi_k \tag{8}$$

which may be solved numerically by setting a "1st guess" $\phi_k = -\varphi' + 2\pi k/N$ in the right side of eq.(8) and recalculate ϕ_k until convergence is obtained.

3. Fields and power calculation

To calculate the power radiated from the collection of charges in Figure 1, one needs only the far fields, i.e. those who behave like $1/R$. The far electric and magnetic fields due to a charge Q moving with non relativistic velocity are given by [2, 7]:

$$\bar{E}_Q = Q\mu_0 \frac{-\bar{a} + (\widehat{R} \cdot \bar{a})\widehat{R}}{4\pi R} \tag{9}$$

and

$$\bar{H}_Q = \widehat{R} \times \bar{E}/\eta_0 = -Q\frac{\widehat{R} \times \bar{a}}{4\pi c R} \tag{10}$$

where $\widehat{R}$ is the unit vector pointing from the charge's position to observer, R is the distance between the charge and the observer (as defined in eq. 2) and $\bar{a}$ is the charge's acceleration. All the dynamical variables are evaluated at the retarded time (defined in eq. 4). The constants $\mu_0 = 1.2566 \times 10^{-6}$H/m and $\eta_0 = 377\Omega$ are the free space permeability and the free space impedance, respectively.

For the collection of charges we need to sum the fields of the individual charges in Figure 1. We first evaluate $\widehat{R}_k \times \bar{a}_k = \bar{R}_k \times \bar{a}_k/R$ for the charge k. For the circular motion $\bar{a}_k = -\omega^2 b \bar{r}'_k$, so that $\bar{R}_k \times \bar{a}_k = (\bar{r} - \bar{r}'_k) \times \bar{a}_k$ which simplifies to. After some algebra we obtain

$$\widehat{R}_k \times \bar{a}_k = \omega^2 b[\widehat{\theta} \sin\phi_k - \widehat{\varphi} \cos\theta \cos\phi_k] \tag{11}$$

In the denominator of eqs. (9) and (10) we may set $R = r$, as always done for far field. So we obtain

$$\bar{H} = \sum_{k=1}^{N} \bar{H}_{Qk} = -\frac{q/N}{4\pi cr}\omega^2 b[\widehat{\theta}\,\mathrm{Fs} - \widehat{\varphi}\cos\theta\,\mathrm{Fc}] \tag{12}$$

where the functions Fs and Fc are defined as

$$\mathrm{Fs}(t, \varphi, \theta, \beta, N) \equiv \sum_{k=1}^{N} \sin\phi_k \tag{13}$$

and

$$\mathrm{Fc}(t, \varphi, \theta, \beta, N) \equiv \sum_{k=1}^{N} \cos\phi_k, \tag{14}$$

Inverting eq. (10) we obtain $\bar{E} - \eta_0 \sum_{k=1}^{N} \widehat{R}_k \times \bar{H}_{Qk}$, but in the far field $\widehat{R}_k$ may be approximated by $\widehat{r}$ so the electric field simplifies to

$$\bar{E} = \mu_0 \frac{q/N}{4\pi r}\omega^2 b[\widehat{\varphi}\,\mathrm{Fs} + \widehat{\theta}\cos\theta\,\mathrm{Fc}] \tag{15}$$

The power per unit of normal area (or Poynting vector) is given by, $\bar{S} = \bar{E} \times \bar{H} = \widehat{r}E^2/\eta_0$ which results in

$$\bar{S} = \widehat{r}\left[\frac{q\omega^2 b}{4\pi cNr}\right]^2 \eta_0 \left|\widehat{\varphi}\,\mathrm{Fs} + \widehat{\theta}\cos\theta\,\mathrm{Fc}\right|^2 \tag{16}$$

The total power is calculated via $P = r^2 \int_0^{2\pi} d\varphi \int_0^{\pi} d\theta \sin\theta \bar{S} \cdot \widehat{r}$ which results in

$$P = \frac{q^2 a^2}{6\pi\epsilon_0 c^3} G(t, \beta, N) \tag{17}$$

where $\omega^2 b$ has been replaced by the charges' acceleration a, and the Larmor formula for the radiation of a single charge has been factored out, so that:

$$G(t, \beta, N) \equiv \frac{3}{8\pi N^2} \int_0^{2\pi} d\varphi \int_0^{\pi} d\theta \sin\theta\, F(t, \varphi, \theta, \beta, N) \tag{18}$$

hence $G = 1$ for $N = 1$, for any t or β and the function F is

$$F(t, \varphi, \theta, \beta, N) \equiv \left|\widehat{\varphi}\,\mathrm{Fs} + \widehat{\theta}\cos\theta\,\mathrm{Fc}\right|^2 = \mathrm{Fs}^2 + \cos^2\theta\,\mathrm{Fc}^2 \tag{19}$$

This allows us to change to variable φ' defined in eq. (6), obtaining for G

$$G(t,\beta,N) = \frac{3}{8\pi N^2}\int_{-\omega(t-r/c)}^{2\pi-\omega(t-r/c)} d\varphi' \int_0^\pi d\theta \sin\theta \, (\mathrm{Fs}^2 + \cos^2\theta \, \mathrm{Fc}^2), \tag{20}$$

We see that if ϕ_k and φ' satisfy eq. (8), also $\phi_k - 2\pi$ and $\varphi' + 2\pi$ satisfy it, hence $\cos\phi_k$ and $\sin\phi_k$ are periodic functions of φ', with a periodicity of 2π. Therefore, the $d\varphi'$ integral in eq. (20) may be evaluated over any period of 2π, showing that G (and therefore also the radiated power P) does *not depend on time*, so that we may simplify eq. (20) to

$$G(\beta,N) = \frac{3}{8\pi N^2}\int_0^{2\pi} d\varphi' \int_0^\pi d\theta \sin\theta \, (\mathrm{Fs}^2 + \cos^2\theta \, \mathrm{Fc}^2). \tag{21}$$

We redefined G to be time independent, and Fs and Fc in eqs. (13) and (14) become functions of φ' instead of t and φ.

For understanding the behavior of Fs and Fc in eqs. (13) and (14) we plot those functions for different parameters, as follows.

Clearly for very small p in eq. (8), $\phi_k \approx -\varphi' + 2\pi k/N$, hence the cosine or sine of ϕ_k equal approximately to the cosine or sine of $-\varphi' + 2\pi k/N$, so that both have harmonic shapes as function of φ'. In such case both the cosines and the sines would sum to 0 because they are separated by phases of $2\pi/N$.

Let us compare the cosines first. As one observes from the (a) panels of Figures 3, 5, 6 and 4, the cosines sum always to some distorted cosine around 0.

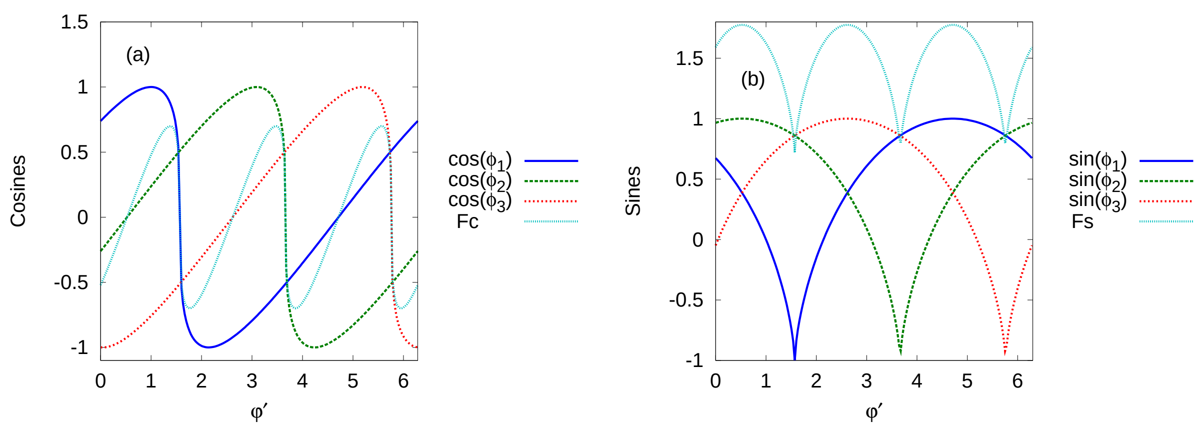

FIG. 3: (color online) The cosines in eq. (14) and their sum is shown in panel (a) and the sines in eq. (13) and their sum is shown in panel (b) for $N = 3$ and $p = 1$.

For $p = 0.5$ the cosines are less distorted from the harmonic shape than for $p = 1$, therefore they sum to values closer to 0, than for the $p = 1$ case. For example, the cosines

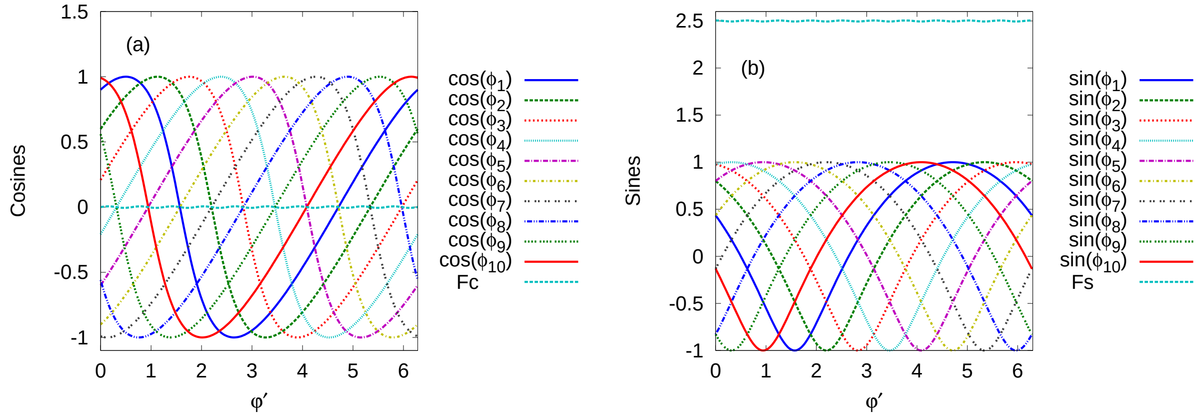

FIG. 4: (color online) The cosines in eq. (14) and their sum is shown in panel (a) and the sines in eq. (13) and their sum is shown in panel (b) for $N = 10$ and $p = 0.5$.

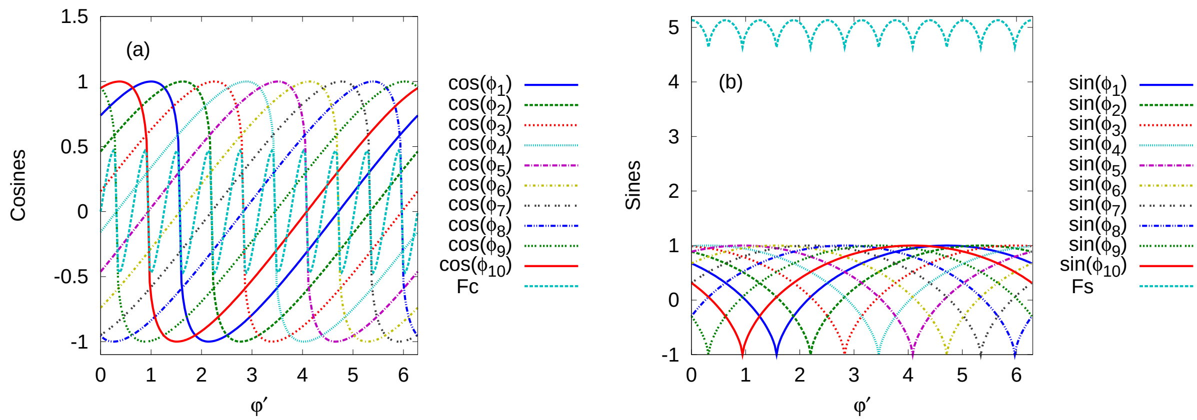

FIG. 5: (color online) The cosines in eq. (14) and their sum is shown in panel (a) and the sines in eq. (13) and their sum is shown in panel (b) for $N = 10$ and $p = 1$.

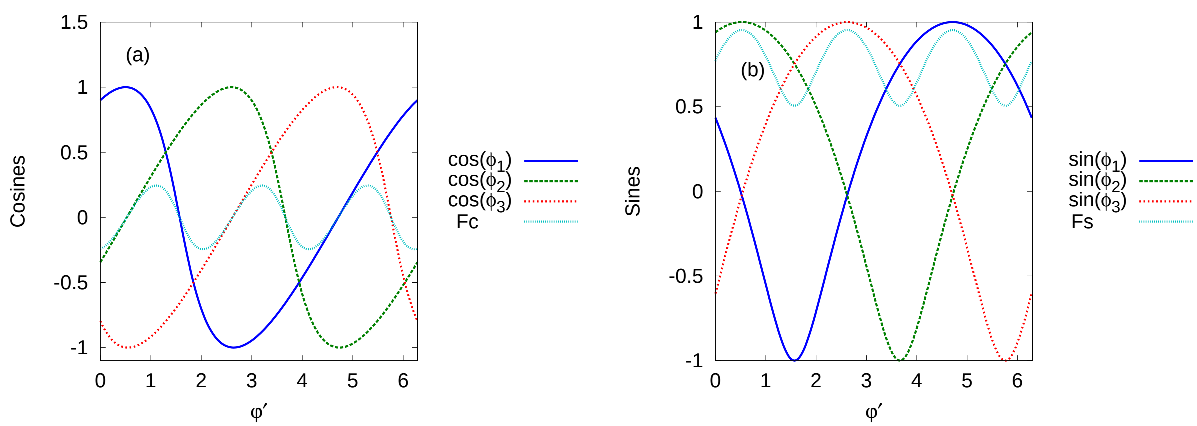

FIG. 6: (color online) The cosines in eq. (14) and their sum is shown in panel (a) and the sines in eq. (13) and their sum is shown in panel (b) for $N = 3$ and $p = 0.5$.

for the case of $p = 0.5$ and $N = 3$ in Figure 6 sum to a distorted cosine of amplitude 0.243 while for the case of $p = 1$ and $N = 3$ in Figure 3 they sum to a distorted cosine of amplitude 0.7 . The effect of the number of charges N is always in lowering the amplitude of the sum of cosines, for example in the case of $p = 0.5$ and $N = 10$ in Figure 4 the amplitude is 0.006 while for the case of $p = 0.5$ and $N = 3$ it is 0.243. To summarize, the cosines sum to higher amplitudes as p gets closer to 1, and sum to lower amplitudes, as N gets bigger, tending to 0 if N tends to infinity.

The behavior of the sines can be understood by looking at Figure 3. The cosines in panel (a) are distorted, so that the negative slope period of each is much shorter than the positive slope period. Therefore the interval in which a sine is negative is much shorted than the interval in which it is positive. Hence the sine functions have a positive "DC level", and therefore sum to a positive value with some ripple. The amplitude of this ripple gets bigger as p gets closer to 1 - for example in the case of $N = 3$ the ripple's amplitude is 1 for the case $p = 1$ and 0.44 for the case $p = 0.5$, but gets smaller as N increases, tending to 0 for N tending to infinity. Therefore the sine functions tend to sum to a constant positive value for $N \to \infty$. This value may be calculated by adding the average values of the sine functions, as follows:

$$\text{Av} = \frac{1}{2\pi} \int_0^{2\pi} d\varphi' \sin \phi_k, \tag{22}$$

and it does not matter for which k we calculate this average. We change variable from φ' to ϕ_k, and we find from eq. (8) that

$$d\varphi'/d\phi_k = -1 - p \ \sin \phi_k, \tag{23}$$

getting:

$$\text{Av} = -\frac{1}{2\pi} \int_{\phi_k(0)}^{\phi_k(0)-2\pi} d\phi_k (1 + p \ \sin \phi_k) \sin \phi_k, \tag{24}$$

where $\phi_k(0)$ is the value of ϕ_k at $\varphi' = 0$. Now the integral $d\phi_k$ of $\sin \phi_k$ over a period of 2π is 0, obtaining:

$$\text{Av} = \frac{p}{2\pi} \int_{\phi_k(0)-2\pi}^{\phi_k(0)} d\phi_k \ \sin^2 \phi_k = \frac{p}{2\pi}\pi = \frac{p}{2} \tag{25}$$

because the integral on $\sin^2\phi_k$ results π. Therefore summing those average values of N charges results in

$$\lim_{N\to\infty} \mathrm{Fs} = \frac{Np}{2} \tag{26}$$

because the ripple's amplitude goes to 0 for big N. For example in the case $N = 3$ and $p = 1$ Figure 3, panel (b) the average value of Fs is 1.5 and for $N = 3$ and $p = 0.5$ (Figure 6) Fs has the average value of 0.75 . For the case $N = 10$ and $p = 0.5$ (Figure 4) Fs has an almost constant value of 2.5 .

Now we continue with the calculation of G in eq. (21). Rewriting eq. (8) for the charge m instead of k results in $\phi_m = -\varphi' + 2\pi m/N + p\,\cos\phi_m$, which may be rewritten as

$$\phi_m = -(\varphi' - 2\pi(m-k)/N) + 2\pi k/N + p\,\cos\phi_m, \tag{27}$$

showing that if we could explicitly express $\phi_k(\varphi')$ from eq. (8), ϕ_m would be the *same* function of φ' only shifted:

$$\phi_k(\varphi') = \phi_m(\varphi' - 2\pi(m-k)/N) \tag{28}$$

as also evident from Figures 3 - 4. Therefore both Fs and Fc functions remain unchanged for a shift of multiples of $2\pi/N$, say:

$$\mathrm{Fc}(\varphi' + 2\pi/N), \theta, \beta, N) = \sum_{k=1}^{N} \cos\phi_k(\varphi' + 2\pi/N) = \sum_{k=1}^{N} \cos\phi_{k+1}(\varphi'). \tag{29}$$

and the sum being on all charges (and k is modulo N), we are left with the same result. We may therefore rewrite in eq. (21)

$$\int_0^{2\pi} d\varphi' = \sum_{n=0}^{N-1} \int_{2\pi n/N}^{2\pi(n+1)/N} d\varphi' \tag{30}$$

and after changing variable $\varphi'' = \varphi' - 2\pi n/N$, we are left with N identical integrals over the period 0 to $2\pi/N$. For simplicity we rename φ'' back to φ' and rewrite the function G as:

$$G(\beta, N) = \frac{3}{8\pi N} \int_0^{2\pi/N} d\varphi' \int_0^{\pi} d\theta \sin\theta \,(\mathrm{Fs}^2 + \cos^2\theta\,\mathrm{Fc}^2), \tag{31}$$

and this will significantly reduce the time of a numerical integration. Now looking at the θ dependence of Fs and Fc, we remark from eq. (8) that ϕ_k depends on $\sin\theta$, hence it is invariant under replacing θ by $\pi-\theta$, and so is $\cos^2\theta$. We may therefore replace the integration from 0 to π by twice the integration from 0 to $\pi/2$, getting

$$G(\beta,N) = \frac{3}{4\pi N}\int_0^{2\pi/N} d\varphi' \int_0^{\pi/2} d\theta \sin\theta\,(\mathrm{Fs}^2 + \cos^2\theta\,\mathrm{Fc}^2), \tag{32}$$

Now we change to the variable p defined in eq. (7) and rewrite eq. (32) obtaining:

$$G(\beta,N) = \frac{3}{4\pi N\beta^2}\int_0^{2\pi/N} d\varphi' \int_0^{\beta} dp\, p\left(\mathrm{Fs}^2/\sqrt{1-(p/\beta)^2} + \mathrm{Fc}^2\sqrt{1-(p/\beta)^2}\right), \tag{33}$$

For the case of $N=1$ one may show analytically that $G=1$ for any β. Fc^2 and Fs^2 reduce to $\cos^2\phi_1$ and $\sin^2\phi_1$ which equal $\frac{1}{2}(1\pm\cos(2\phi_1))$ respectively, and we may perform the $d\varphi'$ integration on Fs^2 or Fc^2 by the change of variable $d\varphi'/d\phi_1$ defined in eq. (23), obtaining

$$\int_0^{2\pi} d\varphi' \frac{1}{2}(1\pm\cos(2\phi_1)) = -\int_{\phi_1(0)}^{\phi_1(0)-2\pi} d\phi_1 (1+p\,\sin\phi_1)\frac{1}{2}(1\pm\cos(2\phi_1)) = \pi \tag{34}$$

which is independent on p, so that one is left with the dp integral in eq. (33), which results $4\beta^2/3$, completing the proof.

For big values of N we know that Fc tends to 0 and Fs tends to $Np/2$ (see eq. (26)), so that we may also obtain an analytical result for $N\to\infty$:

$$\lim_{N\to\infty} G(\beta,N) = \frac{3}{4\pi N\beta^2}\int_0^{2\pi/N} d\varphi' \int_0^{\beta} dp\, p\frac{(Np/2)^2}{\sqrt{1-(p/\beta)^2}} \tag{35}$$

The integrand does not depend on φ', so we obtain:

$$\lim_{N\to\infty} G(\beta,N) = \frac{3}{8\beta^2}\int_0^{\beta} dp\, p\frac{p^2}{\sqrt{1-(p/\beta)^2}}, \tag{36}$$

and the last integral is easily solved by the change of variables $p=\beta\cos\psi$, resulting $2\beta^4/3$. Hence we obtain the final result:

$$\lim_{N\to\infty} G(\beta, N) = \frac{\beta^2}{4} \quad (37)$$

We perform now the calculation in eq. (33) numerically. In this calculation one has to find iteratively ϕ_k in eq. (8) for each value of φ' and p, for values of k between 1 and N. The results are shown as function of N, for different values of β in Figure 7.

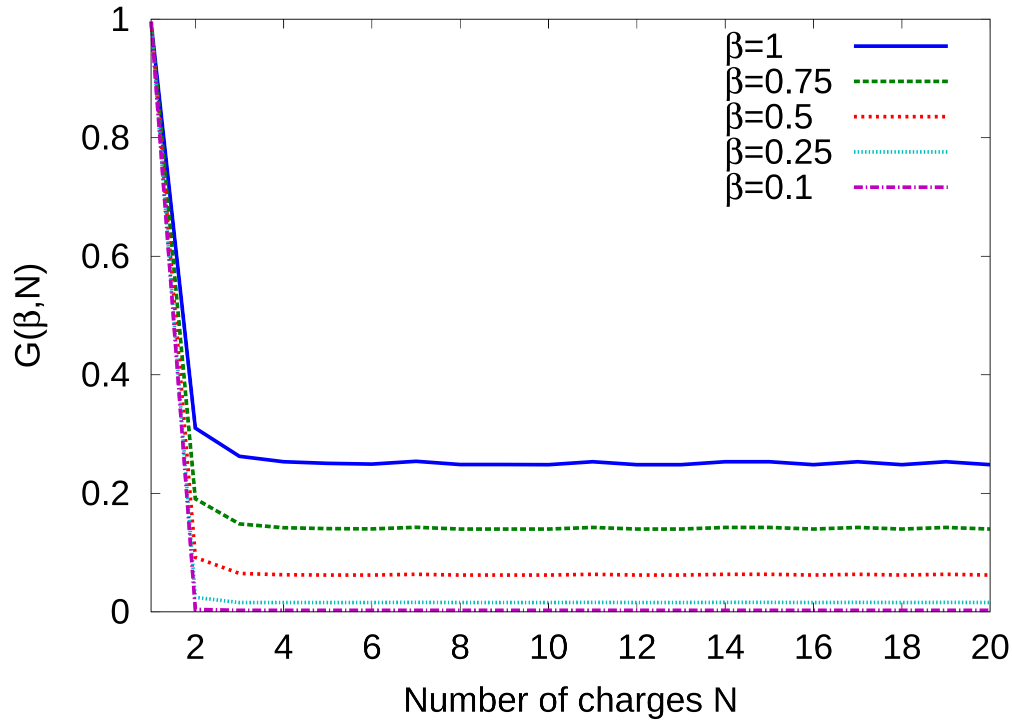

FIG. 7: Result of G (eq. (33)) as function of the number of charges N, for different values of β. For big N we get the asymptotic value $\beta^2/4$ (see eq. (37)).

4. Analysis of the results and examples

The results obtained in the previous section are somehow surprising and unexpected. One expects that for a very big number of charges, the current distribution approaches a continuum DC, and hence the radiated power should go to 0.

However, we will try to interpret the meaning of this result. Looking at the electric field in eq. (15), we see that its $\widehat{\varphi}$ component is proportional to Fs, hence tends to a DC level of $Np/2 = N\beta \sin\theta/2$ for large N, so that it has a large DC level around $\theta = \pi/2$ and goes to 0 for $\theta = 0$ and π. Naturally, the $\widehat{\theta}$ component of the magnetic field in eq. (12) behaves the same way. So for large N the far E and H fields tend to a "DC spherical wave", polarized in the $\widehat{\varphi}$ direction of intensity proportional to $\sin\theta$. But we know there is no such thing as "DC wave", and far $1/R$ depending DC fields. The reason for this anomaly may be explained by looking at the circular source current density, which is in cylindrical coordinates (ρ, φ, z)

$$J_\varphi(\rho, \varphi, z, t) = \frac{qv}{Nb}\delta(z)\delta(\rho - b)\sum_{k=1}^{N}\delta[\varphi - (\omega t + 2\pi k/N)]. \tag{38}$$

In the limit of $N \to \infty$, the δ functions get closer to each other, so that $\sum_{k=1}^{N}\delta[\varphi - (\omega t + 2\pi k/N)]$ should tend to a uniform distribution between $0 < \varphi < 2\pi$ having the area N. Hence this sum should tend to $\frac{N}{2\pi}$, this way obtaining the time independent DC current distribution:

$$J_{\varphi\ \mathrm{DC}}(\rho, \varphi, z) = \frac{qv}{Nb}\delta(z)\delta(\rho - b)\frac{N}{2\pi} = \frac{qv}{2\pi b}\delta(z)\delta(\rho - b) = I_0\delta(z)\delta(\rho - b) \tag{39}$$

where $I_0 = \frac{qv}{2\pi b}$ is the DC current.

However, this mathematical limit of the sum of δ functions does not really exist, so that no matter how big N is, J_φ in eq. (38) remains time dependent, and so do E and H in eqs. (15) and eq. (12).

Another way of understanding this anomaly is by looking at the "self force" which actually is close related to the radiation resistance [4, 5]. As long as the charges are discreet, no matter how close they are to each other, one needs to apply a circular force P/v to rotate them, because they still interact. Only in the continuous case, the charge may rotate by inertia, no need for the circular force.

However, this anomaly arises only for "relativistic velocities", and this work is in the non relativistic framework. For the non relativistic case the results obtained in the previous section seem reliable, and we are going to test them for a current loop of radius $b = 10$ cm, carrying a DC current of 10 Ampers. We take the wire to be copper, having $n = 8.46 \times 10^{28}$ free electrons per cubic meter. We take the cross section radius to be 1 mm so that the cross section is $A = \pi \times 10^{-6}\mathrm{m}^2$. The current can be expressed as $I_0 = enAv$, where $e = 1.6 \times 10^{-19}$ C, so we obtain $v = 2.35 \times 10^{-4}$ m/s, or $\beta = v/c = 7.84 \times 10^{-13}$. The number of charge carriers is so big, that one may use the asymptotic result for $G = \beta^2/4 = 1.54 \times 10^{25}$. The centripetal acceleration is $a = v^2/b = 5.53 \times 10^{-07}\mathrm{m/sec}^2$, so that the radiated power according to eq. (17), using $q = e$ is

$$P|_{\text{10A loop}} = \frac{e^2 a^2}{6\pi\epsilon_0 c^3} G(N \to \infty) = 2.7 \times 10^{-91} \text{watts}. \tag{40}$$

This result is much below any ohmic losses, so it might be verifiable only at 0 Kelvin.

Let us consider another example of DC ion drift in a EHD lifter, as analyzed in [6]. For an application of 22.8 kV to the lifter, it lifted a mass of 13.9 g at least, consuming a current of $I_0 = 0.76$ mA from the power source. The average charge density in this state was $2.265 \times 10^4 \text{C/m}^3$ or dividing by the electron charge, $n = 1.42 \times 10^{15}$ ions per cubic meter. The average cross section of this configuration is $A = 2.5 \times 10^{-3} \text{m}^2$, so expressing again $I_0 = enAv$, we obtain the average velocity of the carriers $v = 1338$ m/sec, or $\beta = v/c = 4.46 \times 10^{-6}$. Alternatively one obtains the same result by multiplying the average electric field which is about half the corona inception field 13.4 MV/m (according to Peek formula - see [6], eq. (32)) by the ion mobility which is $2 \times 10^{-4} \text{m}^2/\text{V sec}$). The average radius of curvature in this configuration is $b = 5$ cm, so we may calculate the average acceleration $a = v^2/b = 35.8 \times 10^6 \text{m/sec}^2$. The big number of carriers justifies the use of the asymptotic result for $G = \beta^2/4 = 4.97 \times 10^{-12}$. So we calculate the radiated power:

$$P|_{\text{lifter}} = \frac{e^2 a^2}{6\pi\epsilon_0 c^3} G(N \to \infty) = 3.62 \times 10^{-50} \text{watts}. \tag{41}$$

which is probably impossible to measure.

CONCLUSIONS

In this work we calculated non relativistically the power radiated by charges in centripetal acceleration. Those charges in the limit of continuous distribution around the motion circle ($N \to \infty$) represent a DC loop. We showed that for charges at high velocity (close to the speed of light) the wave fronts of the individual charges are distorted cosine and sine functions, hence summing to non zero, but the sum decreases as the number of charges increases. However for charges at low velocity the wave fronts are almost undistorted harmonics, hence they sum to zero for very few charges. In the limit of zero velocity, even two charges interfere destructively, their field summing to zero.

Our calculation is non relativistic and shows some anomalies in the relativistic limit.

Those will be cleared out in a future relativistic work, which is ongoing. Also, a quantum analysis to look for the connection between radiation (i.e. radiative electron transition) and electron localization and acceleration would be interesting to carry out.

[1] P.A.M. Dirac, Classical theory of radiating electrons, Proc. Roy. Soc. of London Ser. A **167**, 148-169, (1938)

[2] R. Ianconescu, L.P. Horwitz, Self-force of a classical charged particle, Phys. Rev. A **45** (7), 4346-4354 (1992)

[3] A. Gupta and T. Padmanabhan, Radiation from a charged particle and radiation reaction revisited, Phys. Rev. D **57**, 7241-7250 (1998)

[4] R. Ianconescu, L.P. Horwitz, Self-force of a charge in a real current environment, Found. Phys. Lett. **15** (6), 551-559 (2002)

[5] R. Ianconescu, L.P. Horwitz, Energy Mechanism of Charges Analyzed in Real Current Environment, Found. Phys. Lett. **16** (3), 225-244 (2004)

[6] R. Ianconescu, D. Sohar, M. Mudrik, An analysis of the Brown-Biefeld effect, J. Electrostatics **65** (6), 512-521 (2011)

[7] F. Rhorlich, Classical charged particles, Addison-Wesley, Reading, MA (1990)